Preparation and Properties of Cellulose Nanofibril-graphene Nanosheets/Polyaniline Composite Conductive Aerogels

Hui Zhang,[a] Tianyan Jiang,[a] Xinghua He,[a] Tiantian Chen,[a] Li Fan,[a] Mengxi Gao,[a] and Pengtao Liu [a,b,*]

Polyaniline (PANI) is a conductive polymer that allows cellulose aerogels to achieve high electrical conductivity. However, aerogels containing PANI alone display a low mechanical stability. Graphene nanosheets (GNS) display high conductivity and mechanical strength but are prone to agglomeration, hindering their electroactive sites. To avoid shortcomings of the individual components, a composite aerogel was prepared *via* addition of graphene nanosheets (GNS) and PANI to a suspension of cellulose nanofibril (CNF). Transmission electron microscopy and scanning electron microscopy were used to analyze the structural morphology of the CNF/GNS/PANI aerogel. The electrochemical properties were analyzed using a four-probe conductivity meter, cyclic voltammetry, galvanostatic charge-discharge tests, and electrochemical impedance spectroscopy. A 2:2:1 ratio of CNF/GNS/PANI provided optimal structural and electrochemical results. Incorporation of PANI through *in-situ* polymerization for 6 h resulted in uniform mixing of the three components. The CNF/GNS/PANI composite aerogel displayed a high electrical conductivity with a specific capacitance of 375 Fg^{-1} at a current density of 0.2 Ag^{-1}. As a base binder and dispersant, CNF made use of PANI as a conductive medium and of GNS as a conductive reinforcing medium to form a flexible nanocellulose composite conductive material with increased stability and improved performance.

Keywords: Cellulose; Polyaniline; Graphene; Aerogels; Conductive

*Contact information: a: Tianjin Key Laboratory of Pulp & Paper, Tianjin University of Science and Technology, Tianjin 300457, China; b: State Key Laboratory of Biobased Material and Green Papermaking, Qilu University of Technology, Shandong Academy of Sciences, Jinan 250353, China; *Corresponding author: pengtaoliu@tust.edu.cn*

INTRODUCTION

Cellulose aerogels are a type of environmentally friendly material. They combine the advantages of cellulose regeneration, degradability, thermal properties, and chemical stability with the low density, high porosity, and toughness of aerogels (Fischer *et al.* 2006; Hoepfner *et al.* 2008). With the increased understanding of cellulose aerogels through research and the intensification of the global energy crisis, research on the use of cellulose aerogels has gradually increased. In recent years, cellulose aerogel-based materials with a highly permeable nanoporous three-dimensional network structure have shown significant functionality in the fields of photoelectric sensors and biomedicine (De France *et al.* 2017).

There are two main ways for the cellulose aerogels to achieve electrical conductivity: one uses carbonization (thermal cracking) treatment, which results in the formation of cellulose carbon aerogels, and the other uses composite conductive materials

such as graphene and conductive polymers (Wan *et al.* 2018, 2014). Metal oxides, conductive polymers, and carbon-containing materials have become the electrode materials commonly produced for biomedical applications (Wu *et al.* 2014; Yang *et al.* 2014). However, each electrode material has unique advantages and disadvantages in supercapacitor applications. Some provide a longer life cycle while at the same time having a relatively low specific capacitance (Frackowiak 2007). In contrast, conductive polymer materials with higher specific capacitance due to redox properties have a relatively short life cycle and low mechanical stability (Hu *et al.* 2006; Zhang *et al.* 2011). Metal oxides often have limited applicability due to their high resistance, high cost, and toxicity (Wan 2008).

In recent years, conductive polymers have received particular attention in the field of composites because of their reversible doping/dedoping properties, highly conjugated polymer chains, and controlled conduction mechanisms (Fan *et al.* 2007; Bhadra *et al.* 2009). These unique properties play an important role in technical aspects of materials science. Among various conductive polymers, polyaniline (PANI) is one of the most studied because it is easy to synthesize, provides a stable environment, provides good conductivity, and can achieve unconventional rapid transition of conduction/insulation during doping/de-doping (Wang *et al.* 2009a). However, it undergoes expansion and contraction during doping/de-doping, which limits its cycle life, resulting in mechanical shedding of the electrode, a decline of electrochemical properties, and limitations in practical applications (Xu *et al.* 2012).

In contrast, research has found that graphene is an excellent candidate electrode material. Graphene is a two-dimensional nanomaterial composed of a carbon atoms consisting of overlapping sp2 hybrid orbital forming a hexagonal honeycomb lattice. It has extremely high thermal conductivity, a high specific surface area, high mechanical strength, and excellent electrical and optical properties (Novoselov *et al.* 2004). However, graphene nanosheets (GNS) are prone to agglomeration, hindering their electroactive sites. Therefore, pure graphene electrodes do not exhibit the desired capacitance (Wan *et al.* 2016).

To avoid the shortcomings of each single material in displaying both a good mechanical stability as well as excellent electrochemical properties, researchers are moving towards high-performance composite materials (Lee *et al.* 2008). A combination of PANI and graphene has been used to form a novel composite material by several conventional methods, such as *in-situ* polymerization or physical-mechanical mixing, which have been extensively studied to prepare high-performance materials (Esfandiar *et al.* 2011). Zhang *et al.* prepared a graphene/PANI nanofiber composite as an electrode with an electrochemical capacitance of 480 Fg^{-1} (Zhang *et al.* 2010). Xu *et al.* (2010) prepared PANI/graphene oxide (GO) nanosheets as electrodes. Electrochemical studies have shown that PANI and GO have synergistic effects on the stability compared with single components, with nanocomposites reaching an electrochemical capacitance of 555 Fg^{-1}. Zheng *et al.* (2015) used cellulose nanofibril/reduced graphene oxide/carbon nanotube hybrid aerogels as electrodes, and the resulting flexible supercapacitors exhibited high specific capacitance (*i.e.*, during discharge 252 F g^{-1} at current density 0.5 Ag^{-1}) and significant cycle stability (that is, after 1000 charge-discharge cycles at a current density of 1 Ag^{-1}, more than 99.5% of the capacitance). Wang *et al.* (2009b) prepared a flexible graphene/PANI composite by *in-situ* electro polymerization on graphene paper. The results showed a tensile strength of 12.6 MPa coupled with an electrochemical capacitance of 233 Fg^{-1}. Therefore, its performance is better than many other flexible carbon-based electrodes

currently available. Mao *et al.* (2011) prepared composite materials by *in-situ* polymerization of aniline under acidic conditions. Surfactants were added during the experiment to ensure the dispersion of the graphene in the aqueous phase, and the morphology and electrochemical properties of the two components were well maintained. The composite material obtained a high specific capacitance of 526 Fg^{-1} at a current density of 0.2 Ag^{-1}, with good mechanical stability.

In this study, the authors first prepared nanofibrillated cellulose (or cellulose nanofibril, CNF, according to the ISO classification) and then added a mixture of surfactants and GNS to reduce agglomeration. The uniform dispersion of CNF can help to maintain the separation of adjacent GNS. the optimal ratio of CNF and GNS was first explored, and then the ability of two methods was compared (physical mixing and *in situ* polymerization of PANI) to obtain a layered porous network of mixed aerogel. A layered porous frame provides a large specific surface area and a rich pore structure, creating excellent ion accessibility and transportation potential, leading to a higher power performance (Fernández-Merino *et al.* 2010). The results show that the *in-situ* polymerization method allows a more uniform mixing of the three components. Electrochemical performance studies indicate that a CNF:GNS:PANI (2:2:1) composite aerogel has high specific capacitance and structural stability, which results in great advantages in the field of electrode materials for future energy storage systems.

EXPERIMENTAL

Materials

Bleached hardwood dissolving pulp (Asia Symbol Pulp and Paper Co. Ltd, Rizhao, China), the graphene nanosheets (Tokyo chemical industry Co. Ltd, Tokyo, Japan), hydrochloric acid (HCl, 37%) (Binhua Group Co. Ltd, Binzhou, China), aniline (An), ammonium persulfate (APS), sodium dodecyl sulfate (SDS) (Shanghai Macklin Biochemical Co. Ltd, Shanghai, China), and 2,2,6,6-tetramethylpiperidin-1-oxyl (TEMPO) (Tokyo chemical industry Co. Ltd, Tokyo, Japan) were used in this work. All chemicals were analytical grade and deionized water was used throughout.

Preparation and dispersion of CNF

The raw fiber material was subjected to a dehydration and beating pretreatment, and then the product was placed in a $Na_2CO_3/NaHCO_3$ buffer solution, followed by oxidization in a TEMPO/NaClO/NaBr system. The oxidized cellulose was dialyzed until the pH was neutral. Finally, CNF was obtained by high-pressure homogenization (Saito *et al.* 2007; Besbes *et al.* 2011).

Preparation of CNF/GNS aerogels

A reaction mixture was prepared containing solid graphene and CNF at various mass ratios (20%, 30%, 40%, 50%, and 60% graphene). The suspension was stirred with a magnetic stirrer for 2 h, and then ultrasonicated for 1 h using an ultrasonic wave cell breaker at 600 W. Next, the mixture was frozen in liquid nitrogen, and finally freeze-dried to obtain a CNF/GNS composite aerogel. The composite electrode sheet was obtained by tableting the aerogel under a pressure of 0.1 MPa.

Preparation of CNF/GNS/PANI Aerogels

Physical mechanical mixing method

The CNF was prepared as a suspension with a concentration of 1% (w/v). The GNS and SDS were placed into a suspension that was uniformly mixed by ultrasonication for 2 h. The two suspensions were mixed, stirred with a magnetic stirrer for 2 h, and then PANI was gradually added to the suspension in small portions so that the final mass ratio in the mixed system was CNF:PANI:GNS = 2:1:2. The composite electrode sheet was obtained after freezing in liquid nitrogen, freeze drying for 48 h, and tableting under a pressure of 0.1 MPa.

In situ polymerization method

As illustrated in Fig. 1, according to the above method, CNF and GNS were mixed and dispersed at a mass ratio of 1:1, uniformly mixed by stirring on a magnetic stirrer for 2 h. Next, 10 mL of HCl and 25 mg of aniline were added to the mixture, and then magnetic stirring was continued for 1 h. Subsequently, 60 mg of ammonium persulfate was added to 50 mL of 0.5 mol/L HCl solution, and then it was gradually added dropwise to the above mixture. The polymerization was allowed to proceed at 0 °C for 2 h, 3 h, 4 h, 6 h, or 8 h after which the mixture was filtered under vacuum, washed, pre-frozen with liquid nitrogen, and then dried in a freeze-dried dryer for 48 h and pressed at a pressure of 0.1 MPa to obtain a composite electrode sheet.

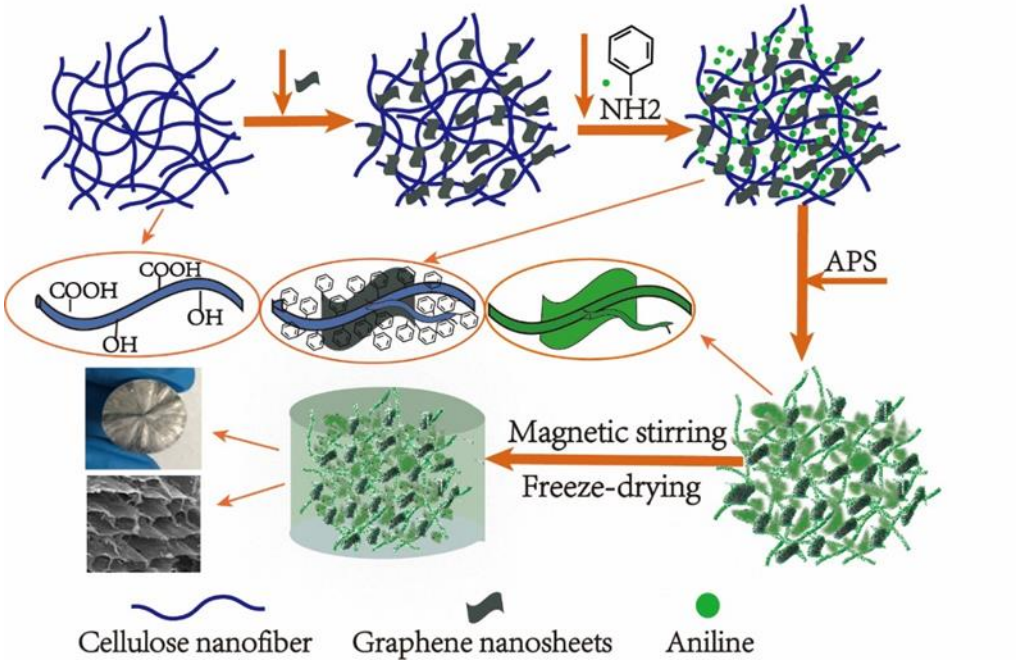

Fig. 1. Preparation of CNF/GNS/PANI composite aerogels by the *in situ* polymerization method

Methods

Characterization of CNF/GNS/PANI composite aerogels

The structure and morphology of the of CNF/GNS/PANI composite aerogels were characterized by transmission electron microscopy (TEM) (JEOL-2010; JEOL Japan Electronics Co. Ltd, Tokyo, Japan), energy dispersive spectrometer (EDS) (GeminiSEM300; Carl Zeiss AG, Berlin, Germany), electronic universal tester (TMC4503;

Jinan hengsi Shanda Instrument Co. Ltd, Jinan, China), Fourier transform infrared spectrometer (FT-IR) (IRTracer-10; Shimadzu Co. Ltd, Tokyo, Japan), specific surface area pore size analyzer (Autosorb-iQ-XR; Quantachrome, USA), and scanning electron microscopy (SEM) (JSM-IT300LV; JEOL Japan Electronics Co. Ltd, Tokyo, Japan). Electrochemical characterization was performed using a four-probe conductivity meter (RTS-8; Suzhou lattice Electronics Co. Ltd, Suzhou, China), electrochemical workstation (CHI650E; Shanghai Chenhua Instrument Co. Ltd, Shanghai, China) for cyclic voltammetry (CV), galvanostatic constant current charge-discharge (GCD) technology, and electrochemical impedance spectroscopy (EIS). The potential range measured by CV was -0.2 to 0.8 V. The GCD voltage window ranged from 0 V to 0.8 V, the segment was set to 4, and the current density range was set from 0.2 A/g to 1 A/g. The EIS initial potential was set to open circuit voltage, the frequency range was set from 0.01 Hz to 100000 Hz. The three-electrode setting was used, where the composite material was used as the working electrode, the platinum electrode was used as the counter electrode, the calomel electrode was used as the reference electrode, and a 1.0 M H_2SO_4 solution was used as the electrolyte.

RESULTS AND DISCUSSION

Morphological and Structural Characterization

Figure 2 shows a transmission electron micrograph of CNF. The Na_2CO_3/$NaHCO_3$ buffer system provided a relatively stable pH environment for the oxidation reaction, thereby improving the selectivity of the TEMPO-dependent catalytic oxidation. There was no obvious agglomeration of CNF, the size and distribution of the fibers were relatively uniform, with a good dispersion.

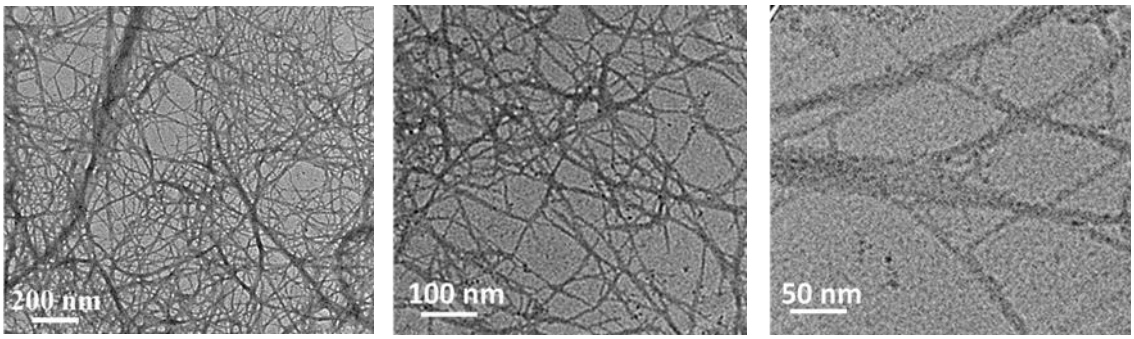

Fig. 2. TEM of CNF showing no obvious agglomeration, uniform fiber distribution, and good dispersion

Figure 3 shows the effect of SDS on the dispersion of graphene. The SDS acted as a surfactant for GNS that still allowed GNS to be evenly dispersed in water after 24 h (vial b). In the absence of SDS, the GNS solution was completely stratified after 6 h (vial a). Thus, SDS provided a stable environment for the three composites and reduced the agglomeration of GNS.

In the composite system, the pore structure is associated with the graphene content, and the optimum ratio of GNS:CNF was experimentally explored. Figure 4 shows the pore structure when GNS:CNF was 1:1 (panel a and b), and the state of the structure when GNS:CNF was 3:2 (panel c and d). It can be seen from Fig. 4 that an increase in the

GNS:CNF ratio from 1:1 to 3:2 led to a loosening of the structure, characterized by suboptimal pore formation and mechanical strength. Therefore, the optimal ratio of GNS:CNF for the structure of the composite aerogel is 1:1.

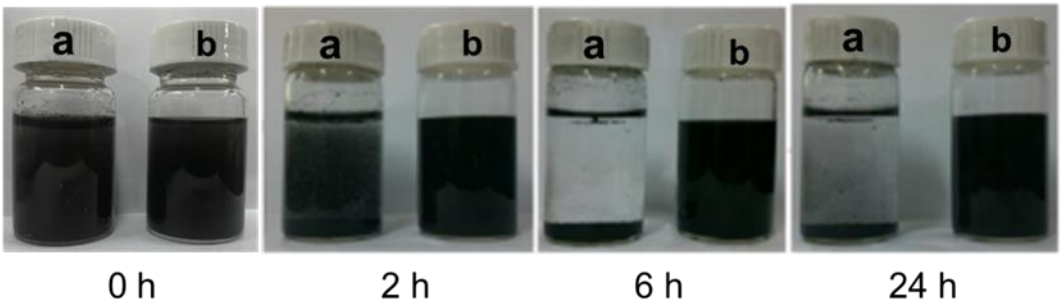

Fig. 3. Effect of SDS on the distribution of GNS (a: graphene without SDS; b: graphene with SDS)

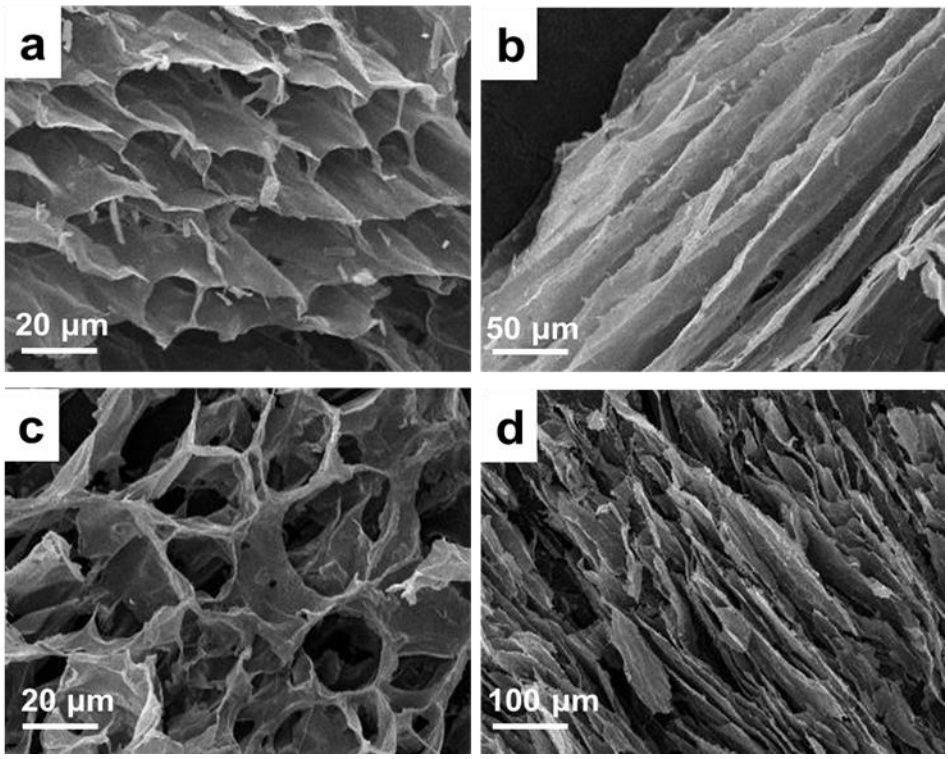

Fig. 4. SEM image of CNF/GNS composite aerogel structure (a) and (b) where GNS: CNF = 1:1; (c) and (d) GNS: CNF = 3:2

In-situ polymerization combines aniline doping with CNF and GNS to form polyaniline. Figure 5 shows the FT-IR spectra of the CNF, GNS, PANI, and CNF/GNS/PANI composites. For CNF, three characteristic peaks at 1061, 1615 and 2903 cm^{-1} indicate the presence of a hydroxyl group and a carboxyl group. For GNS, three characteristic peaks at 1176, 1400, and 1635 cm^{-1} represent the bending vibration peak of -OH, the stretching vibration peak of the secondary alcohol, and the deformation vibration peak of the benzene ring. For pure PANI, the peaks at 1592 and 1498 cm^{-1} correspond to the characteristic C-C extensions of the oxime and benzene rings, respectively, and the

peaks at 1304 and 1145 cm^{-1} are related to the C-N and C=N stretching vibrations. The prepared CNF/GNS/PANI complex has obvious characteristic peaks of GNS and PANI, and the peak intensity is weakened, indicating that the interaction between the three is tight.

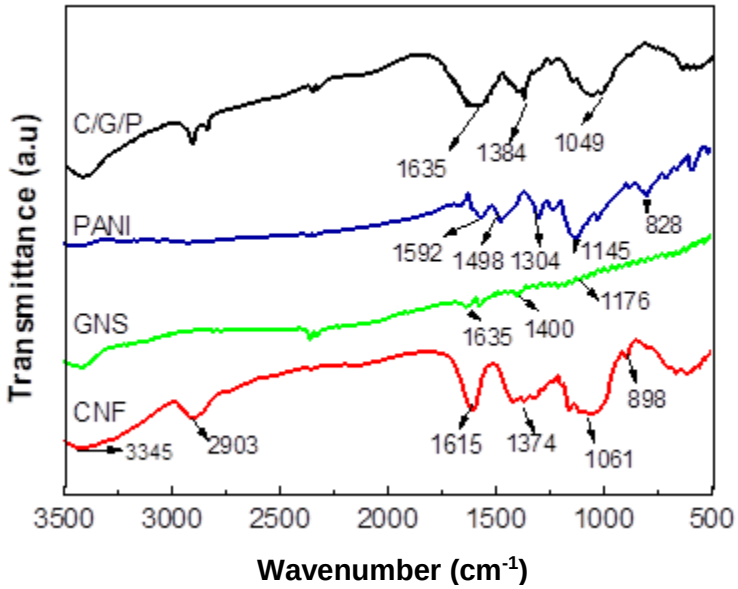

Fig. 5. FT-IR spectrum of CNF, GNS, PANI and *in-situ* polymerized composite aerogel

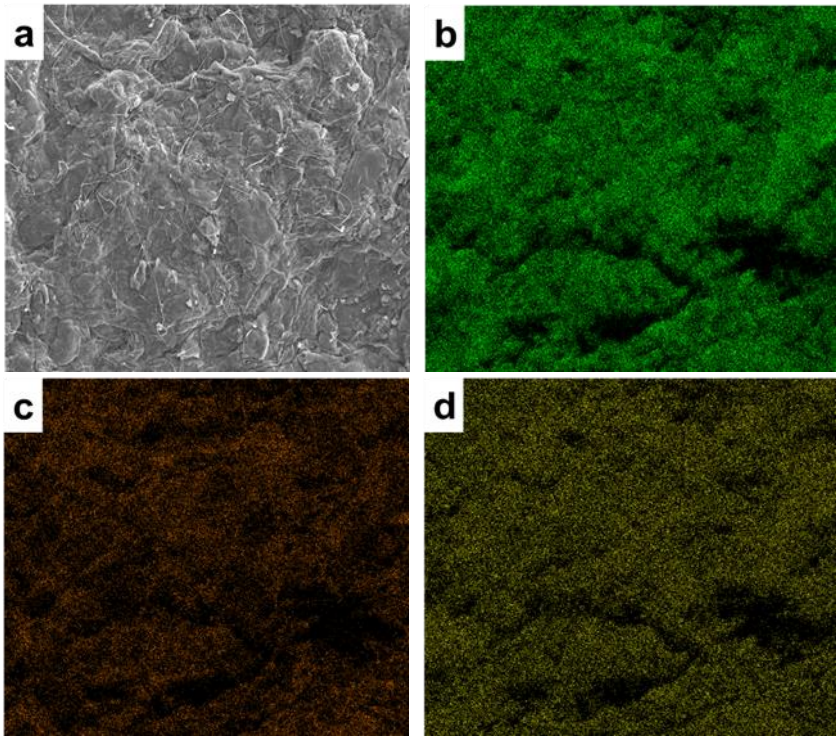

Fig. 6. The SEM image of (a) *In-situ* polymerized composite aerogel; the element mapping images of (b) C atom, (c) O atom and (d) N atom

The analysis of EDS showed that the distribution points of C, O, and N elements in the composite aerogel prepared by in situ polymerization were very close, indicating that

CNF, GNS, and PANI were distributed uniformly in the composite. Based on the analysis results of the above infrared spectrum, it is shown that the PANI formed by in situ polymerization is tightly combined with CNF and GNS.

Composite aerogels prepared by two different methods (*i.e.*, mechanical mixing *vs. in-situ* polymerization) also differ in morphology. Figure 7 shows agglomeration of PANI on the surface (red ellipse in panel b) and on the inside (red ellipse in panel a) of the aerogel prepared by mechanical mixing, displaying a loose structure. In contrast, the aerogel prepared by the *in-situ* polymerization method had a regular pore structure, and PANI agglomeration rarely occurred. Thus, the aerogel obtained by the *in-situ* polymerization method was of superior quality.

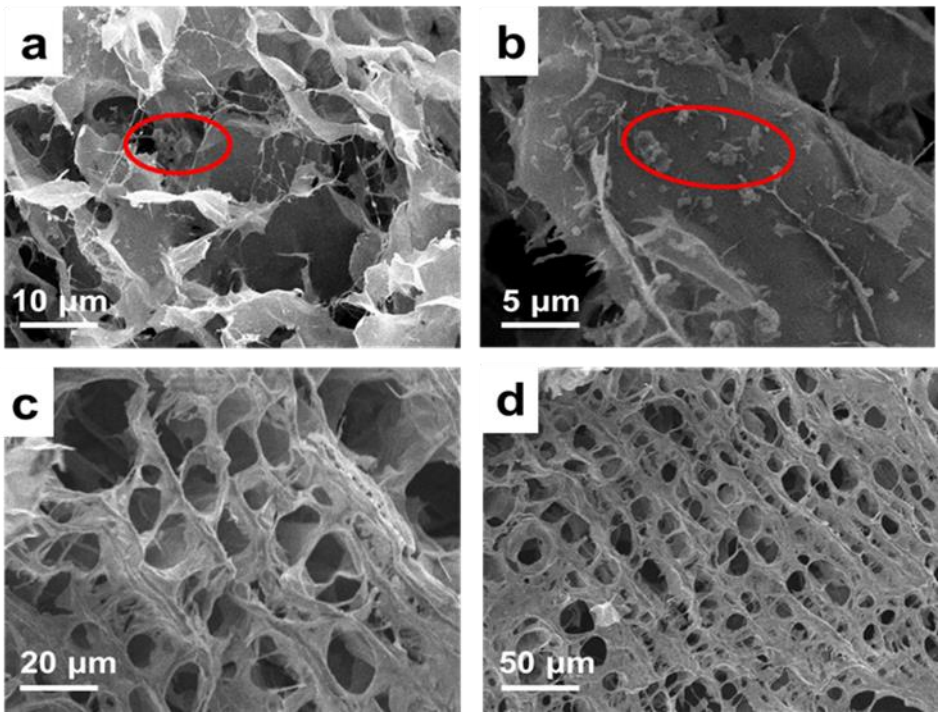

Fig. 7. SEM images of composite aerogel prepared by mechanical mixing (a) and (b) or by *in-situ* polymerization (c) and (d)

The isotherms of the prepared composite aerogels belong to type IV, which is indicative of a mesoporous material, and the pore size was mostly between 5 and 20 nm. The aerogel prepared by in-situ polymerization had a larger adsorption capacity and a more uniform pore size distribution, mainly between 2 and 10 nm. The specific surface area of the mechanically-mixed composite aerogel was 65.1 m^2/g, while the material resulting from *in-situ* polymerization reached 134.2 m^2/g.

When GNS was added at 50%, it provided better compressive properties. The compressive stress could reach 1.9 MPa, indicating a high mechanical strength, which is consistent with the results of SEM image analysis. Compared with the mechanical mixing method, the in-situ polymerization method has obvious advantages. The compression strain can reach 2.35 MPa, which has higher mechanical strength, which is consistent with the above analysis.

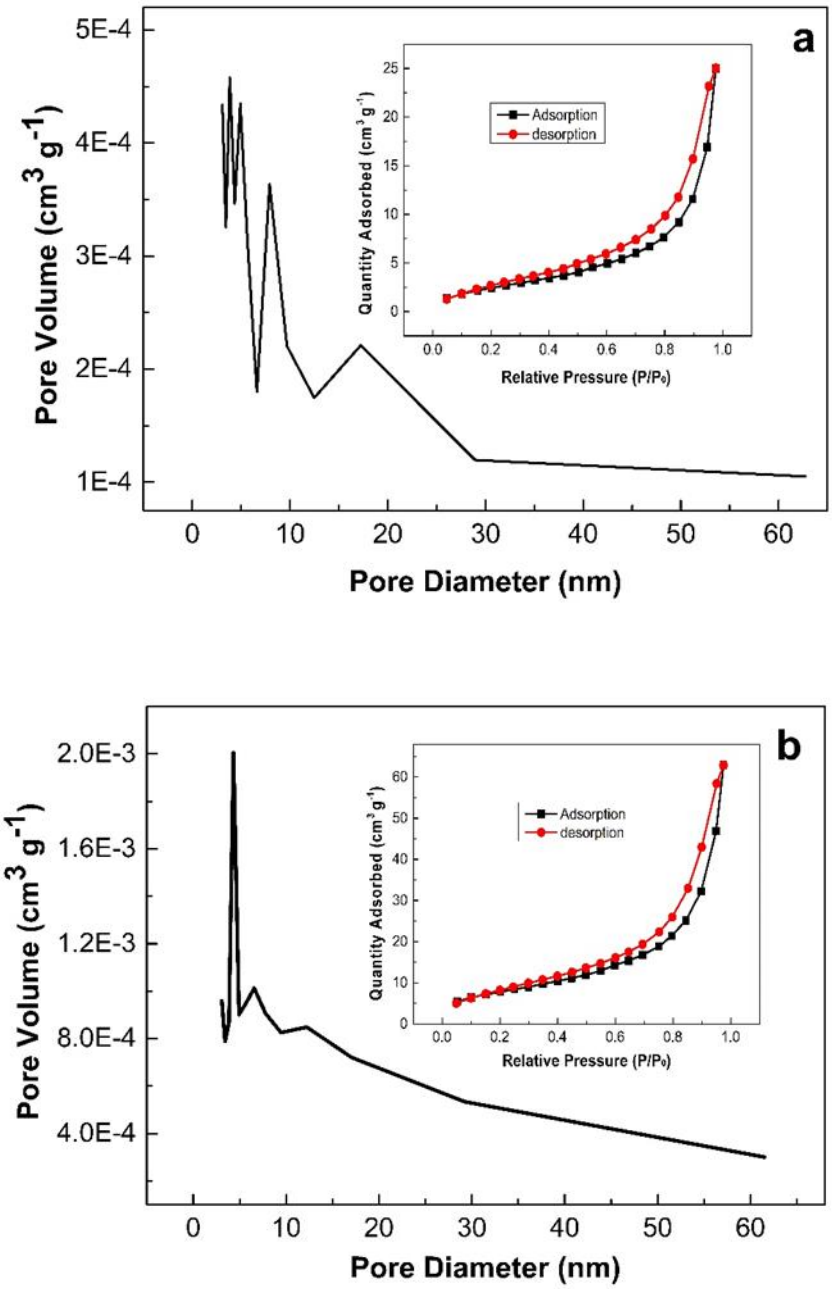

Fig. 8. N_2 adsorption-desorption isotherm and pore diameter analysis of composite aerogels (a) mechanical mixing method; (b) *in situ* polymerization method

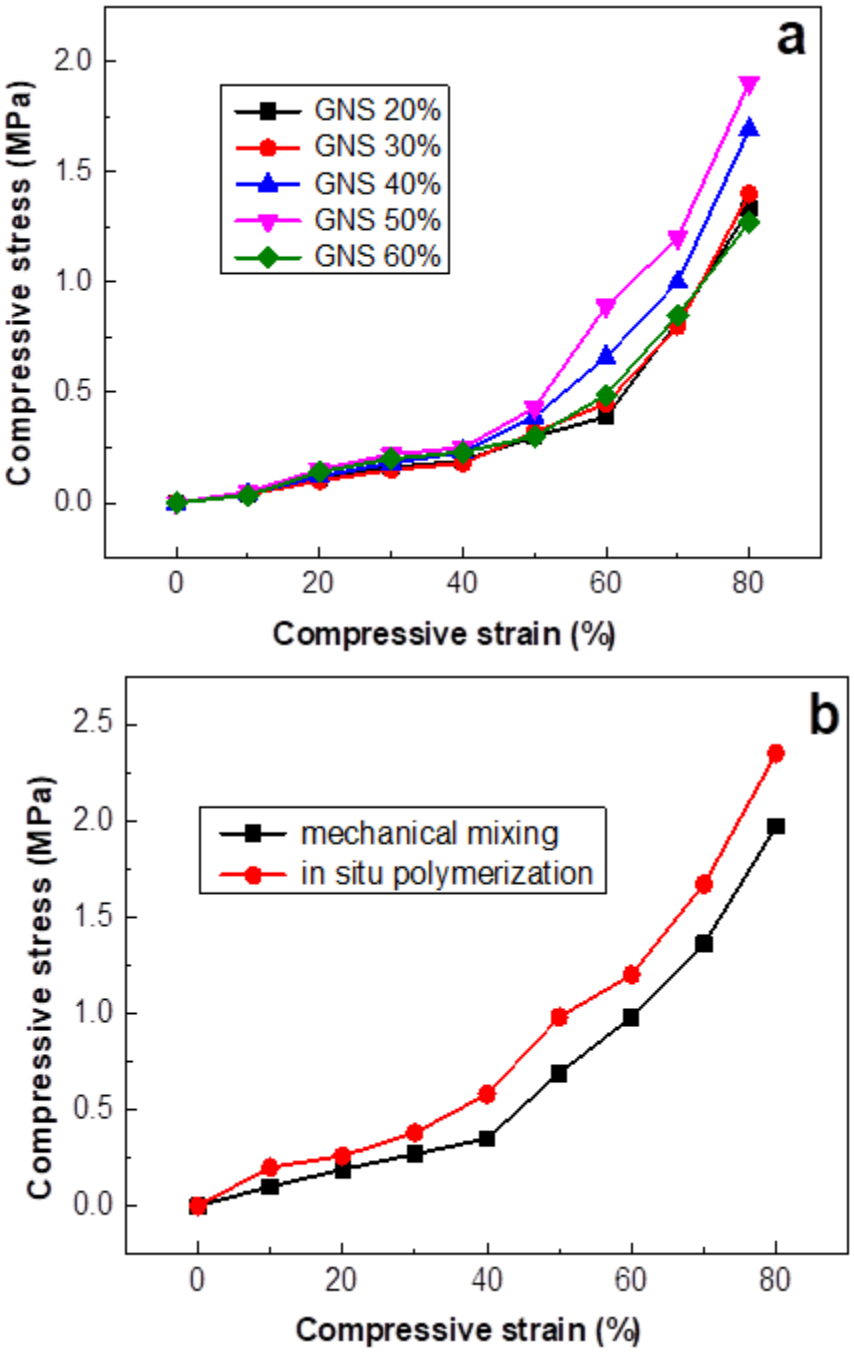

Fig. 9. Stress-strain curve of the composite aerogel (a) different GNS content; (b) different preparation methods

Electrochemical Characterization

The conductivity of the electrode sheets was measured using a four-probe conductivity meter. The measurement points were (0, 0), (0, 1), (0, -1), (1, 0), and (-1, 0), and the average conductivity of each electrode was obtained. As shown in Fig. 10, as the percentage of GNS increased, the average conductivity of the electrode also increased. When the GNS content exceeded 50%, the electrical conductivity still increased (to 7.21 S/cm at 60% GNS), but the surface structure of the electrode was loosened and the GNS

fell off, resulting in the loss of active material. Therefore, the authors found that when the GNS:CNF ratio was 1:1, the dispersion and mechanical properties were optimal.

Figure 11 shows that as the *in-situ* polymerization time of PANI increased, the average conductivity of the electrode also gradually increased. When the polymerization time was 6 h, the conductivity reached a maximum of 11.78 S/cm. When the polymerization time exceeded 6 h, the conductivity decreased. In an oxidizing environment, the excessive polymerization time of aniline caused oxidative degradation of the formed molecular chain, thereby reducing its electrical conductivity.

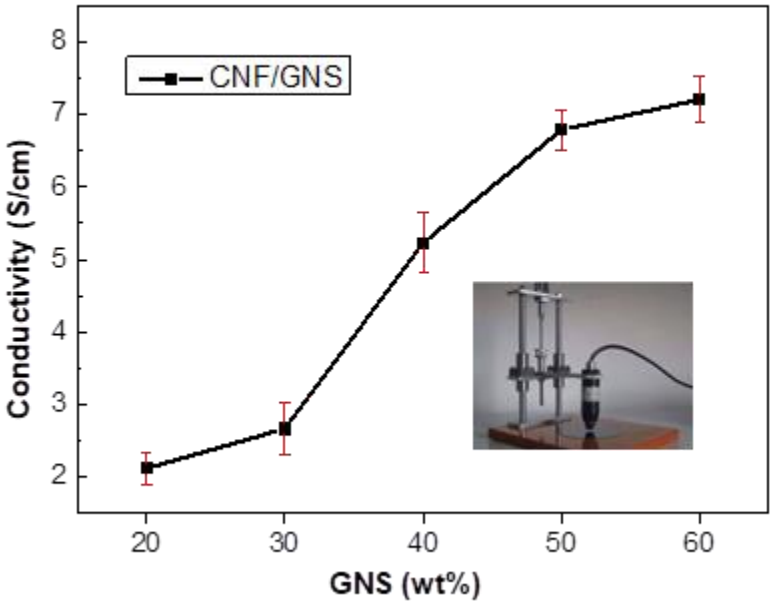

Fig. 10. Conductivity test of composite electrode with different CNF/GNS ratios

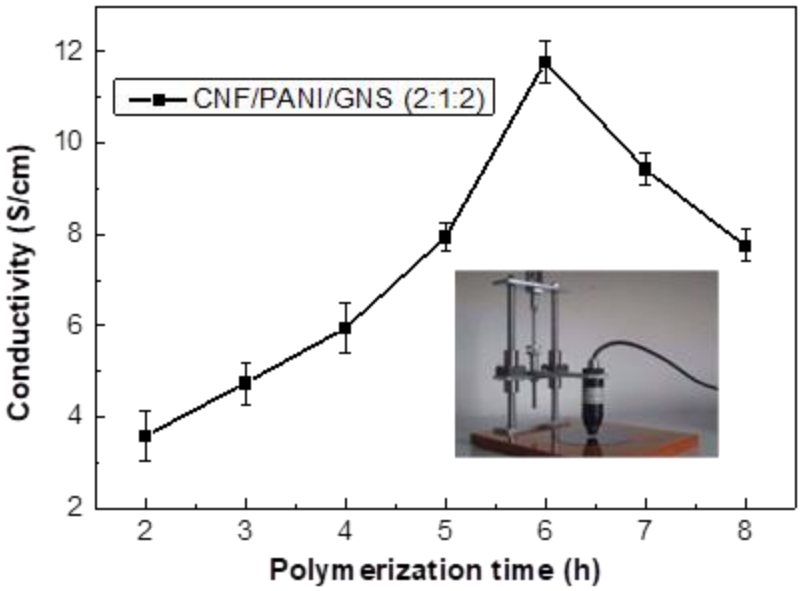

Fig. 11. Effect of different *in-situ* polymerization times of PANI on the conductivity of CNF/PANI/GNS (2:1:2) aerogels

Based on the cyclic voltammetry curve and the mass of the active material on the electrode, the specific capacitance of the electrode material can be calculated by Eq. 1,

$$C_{cv} = \frac{\int IdV}{v\Delta Vm} \quad (1)$$

where C_{cv} is the specific capacitance of composite materials (F/g), I is the current (A), V is the potential window (V), m is the mass of the active material on the electrode (g), and v is the canning speed (mV/s).

The specific capacity of the composite material can also be calculated according to Eq. 2,

$$C_{cd} = \frac{It}{m\Delta V} \quad (2)$$

where C_{cd} is the specific capacity of the electrode material (F/g), I is the current (A), t is the discharge time (s), V is the voltage difference after IR drop (V), and m is the active material on the electrode quality (g).

Figure 12 shows that the cyclic volt-ampere curves of different scan rates displayed a rectangular shape, which means that the internal resistance of the composite electrode was small, and that the power characteristics were good. There was no obvious redox peak, which indicated that the composite electrode had good capacitance characteristics and reversibility. The specific capacitances of the composite electrode at the scan rates of 5, 10, 30, 50, and 100 mV/s were calculated using Eq. 1 to be 437.5, 325.6, 241.8, 215.2, and 183.7 F/g, respectively.

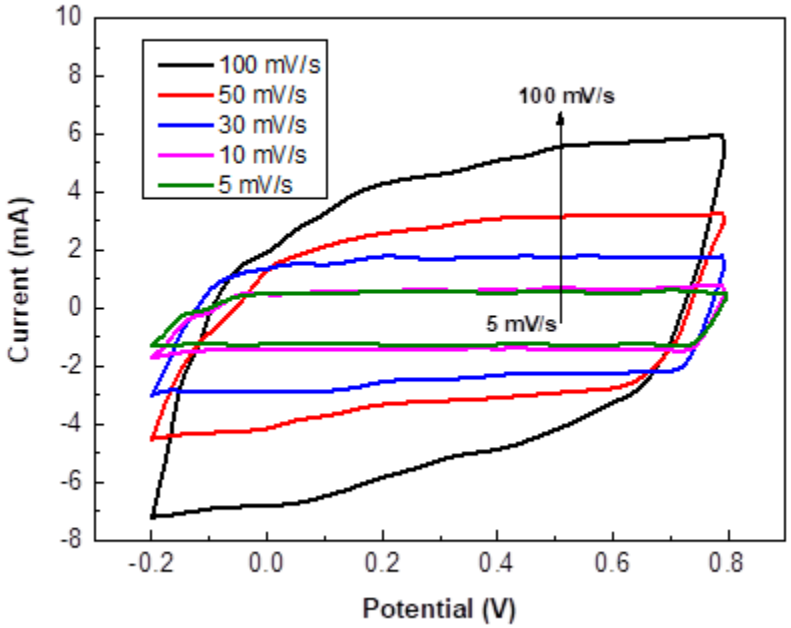

Fig. 12. Effect of scan rates on the cyclic volt-ampere curves of the composite aerogel electrode

The rectangular shape indicated small internal resistance of the composite electrode. Absence of redox peak indicated that the composite electrode had good capacitance characteristics and reversibility.

The charge-discharge curves exhibited a triangular characteristic at different current densities (Fig. 13), which indicated that the voltage of the electrode had a linear relationship with the charge and discharge time and exhibited good charge and discharge performance. There was a small pressure drop at the beginning of the discharge, indicating that the internal resistance of the composite electrode was small. The specific capacitances of the composite electrodes at current densities of 0.2, 0.3, 0.5, and 1 A/g were calculated by Eq. 2 to be 375, 283, 208, and 169 F/g, respectively.

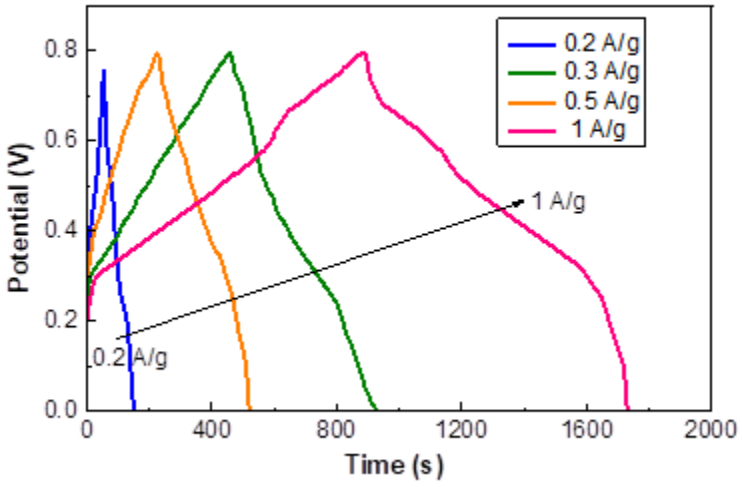

Fig. 13. Galvanostatic charge-discharge (GCD) of composite aerogel electrode at various current densities

The EIS initial potential was set to open circuit voltage, and the frequency range was set from 0.01 Hz to 100000 Hz. The CNF/GNS/PANI aerogel was the working electrode, the platinum electrode was the counter electrode, and the calomel electrode was the reference electrode. 1.0 M H_2SO_4 was the electrolyte. Above 80 ohm the curve was almost perpendicular to the Z' axis, indicating that the composite electrode had excellent capacitance properties. Figure 14 shows that as the Z' axis increased continuously, the curve in the figure had three stages of changes.

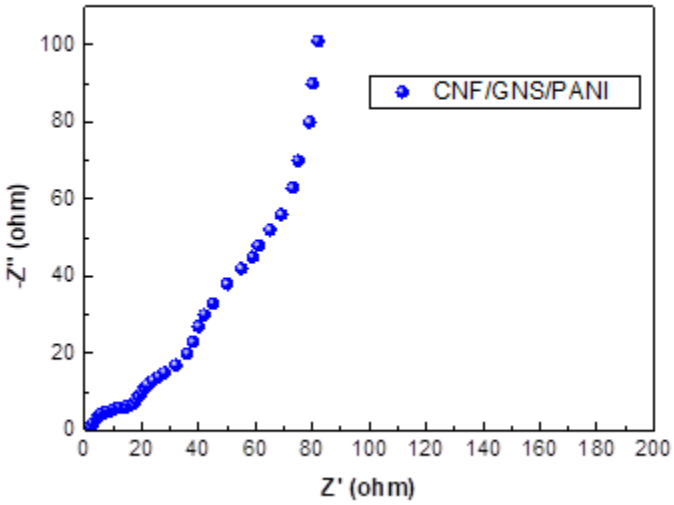

Fig. 14. Nyquist plot for the composite CNF/GNS/PANI aerogel electrode

The first segment was semicircular, indicating the high frequency region of the electrode. The second segment was a straight line with a slope of approximately 45°, corresponding to the intermediate frequency region. The third segment was a straight line approximately parallel to the Z'' axis, corresponding to the low frequency region of the electrode. The internal resistance of the electrolyte was 15.8 Ω. A line almost perpendicular to the Z' axis indicates that the composite electrode has excellent capacitance properties.

CONCLUSIONS

1. SEM images and pore size distributions analysis revealed that *in situ* polymerization of aniline caused polyaniline (PANI) to be uniformly dispersed on the inside and surface of aerogels comprised of nanofibrillated cellulose (CNF), graphene nanosheets (GNS) and PANI, retaining the original loose porous structure. Compared with the mechanical mixing method, it had higher compressive stress.
2. Tests on its different electrochemical properties showed that CNF/GNS/PANI composite electrodes had excellent electrical conductivity and were suitable as electrode materials.
3. Both GNS and CNF formed a three-dimensional network, which provided a stable basic support for PANI. In summary, the three composite CNF/GNS/PANI aerogels are excellent electrode materials that are ideal for supercapacitors.

ACKNOWLEDGMENTS

The financial support for this project was from the National Key Research and Development Plan (No. 2017YFB0307902), the National Nature Science Foundation of China (No. 21576213), the Scientific Research Project of Tianjin Municipal Education Commission (No. 2018KJ098), the Foundation of State Key Laboratory of Biobased Material & Green Papermaking (No. KF201809), and the Young Teachers' Innovation Fund of Tianjin University of Science and Technology (No. 2017LG06).

REFERENCES CITED

Besbes, I., Alila, S., and Boufi, S. (2011). "Nanofibrillated cellulose from tempo-oxidized eucalyptus fibres: Effect of the carboxyl content," *Carbohyd. Polym.* 84(3), 975-983. DOI: 10.1016/j.carbpol.2010.12.052

Bhadra, S., Khastgir, D., Singha, N. K., and Lee, J. H. (2009). "Progress in preparation, processing and applications of polyaniline," *Prog. Polym. Sci.* 34(8), 783-810. 10.1016/j.progpolymsci.2009.04.003

De France, K. J., Hoare, T., and Cranston, E. D. (2017). "Review of hydrogels and aerogels containing nanocellulose," *Chem. Mater.* 29(11), 4609-4631. DOI: 10.1021/acs.chemmater.7b00531

Esfandiar, A., Akhavan, O., and Irajizad, A. (2011). "Melatonin as a powerful bio-antioxidant for reduction of graphene oxide," *J. Mater. Chem.* 21(29), 10907-10914. DOI: 10.1039/C1JM10151J

Fischer, F., Rigacci, A., Pirard, R., Berthon-Fabry, S., and Achard, P. (2006). "Cellulose-based aerogels," *Polymer* 47(22), 7636-7645. DOI: 10.1016/j.polymer.2006.09.004

Frackowiak, E. (2007). "Carbon materials for supercapacitor application," *Phys. Chem. Chem. Phys.* 9(15), 1774-1785. DOI: 10.1039/b618139m

Fan, L. Z., Hu, Y. S., Maier, J., Adelhelm, P., Smarsly, B., and Antonietti, M. (2007). "High electroactivity of polyaniline in supercapacitors by using a hierarchically porous carbon monolith as a support," *Adv. Funct. Mater.* 17(16), 3083-3087. 10.1002/adfm.200700518

Fernández-Merino, M. J., Guardia, L., Paredes, J. I., Villar-Rodil, S., Solís-Fernández, P., Martínez-Alonso, and Tascón, J. M. D. (2010). "Vitamin C is an ideal substitute for hydrazine in the reduction of graphene oxide suspensions," *J. Phys. Chem.* C 114(14), 6426-6432. DOI: 10.1021/jp100603h

Hoepfner, S., Ratke, L., and Milow, B. (2008). "Synthesis and characterisation of nanofibrillar cellulose aerogels," *Cellulose* 15(1), 121-129. DOI: 10.1007/s10570-007-9146-8

Hu, C. C., Chang, K. H., Lin, M. C., and Wu, Y. T. (2006). "Design and tailoring of the nanotubular arrayed architecture of hydrous RuO_2 for next generation supercapacitors," *Nano Lett.* 6(12), 2690-2695. DOI: 10.1021/nl061576a

Lee, C., Wei, X., Kysar, J. W., and Hone, J. (2008). "Measurement of the elastic properties and intrinsic strength of monolayer graphene," *Science* 321(5887), 385-388. DOI: 10.1126/science.1157996

Mao, L., Zhang, K., Chan, H. S. O., and Wu, J. (2011). "Surfactant-stabilized graphene/polyaniline nanofiber composites for high performance supercapacitor electrode," *J. Mater. Chem.* 22(1), 80-85. DOI: 10.1039/C1JM12869H

Novoselov, K. S., Geim, A. K., Morozov, S. V., Jiang, D., Zhang, Y., Dubono, S. V., Grigorieva, I. V., and Frisov, A. A. (2004). "Electric field effect in atomically thin carbon films," *Science* 306(5696), 666-669. DOI: 10.1126/science.1102896

Saito, T., Kimura, S., Nishiyama, Y., and Isogai, A. (2007). "Cellulose nanofibers prepared by tempo-mediated oxidation of native cellulose," *Biomacromolecules* 8(8), 2485-2491. DOI: 10.1021/bm0703970

Wang, D., Huang, J., Lan, W., and Li, X. (2009a). "Neural network-based robust adaptive control of nonlinear systems with unmodeled dynamics," *Math. Comput. Sim.* 79(5), 1745-1753. DOI: 10.1016/j.matcom.2008.09.002

Wang, D. W., Li, F., Zhao, J., Ren, W., Chen, Z. G., and Tan, J., Wu, Z. S., Gentle, I., Lu, G. Q., and Cheng, H. M. (2009b). "Fabrication of graphene/polyaniline composite paper via in situ anodic electropolymerization for high-performance flexible electrode," *ACS Nano* 3(7), 1745-1752. DOI: 10.1021/nn900297m

Wan, M. (2008). "A template-free method towards conducting polymer nanostructures," *Adv. Mater.* 20(15), 2926-2932. DOI: 10.1002/adma.200800466

Wan, C., Lu, Y., Jiao, Y., Jin, C., and Li, J. (2014). "Fabrication of hydrophobic, electrically conductive and flame-resistant carbon aerogels by pyrolysis of regenerated cellulose aerogels," *Carbohyd. Polyme.* 118C. DOI: 10.1016/j.carbpol.2014.11.010

Wan, C., and Li, J. (2016). "Graphene oxide/cellulose aerogels nanocomposite: Preparation, pyrolysis, and application for electromagnetic interference shielding," *Carbohyd. Polym.* S0144861716305732. DOI: 10.1016/j.carbpol.2016.05.051

Wan, C., Jiao, Y., Wei, S., Zhang, L. Y., and Wu, Y. Q. (2018). "Functional nanocomposites from sustainable regenerated cellulose aerogels: A review," *Chem. Eng. J.* 359, 459-475. DOI: 10.1016/j.cej.2018.11.115

Wu, W., Li, Y., Yang, L., Ma, Y., Pan, D., and Li, Y. (2014). "A facile one-pot preparation of dialdehyde starch reduced graphene oxide/polyaniline composite for supercapacitors," *Electrochim. Acta* 139, 117-126. DOI: 10.1016/j.electacta.2014.06.166

Xu, G., Wang, N., Wei, J., Lv, L., Zhang, J., Chen, Z., and Xu, Q. (2012). "Preparation of graphene oxide/polyaniline nanocomposite with assistance of supercritical carbon dioxide for supercapacitor electrodes," *Ind. Eng. Chem. Res.* 51(44), 14390-14398. DOI: 10.1021/ie301734f

Xu, J., Wang, K., Zu, S. Z., Han, B. H., and Wei, Z. (2010). "Hierarchical nanocomposites of polyaniline nanowire arrays on graphene oxide sheets with synergistic effect for energy storage," *ACS Nano* 4(9), 5019-5026. DOI: 10.1021/nn1006539

Yang, F., Xu, M., Bao, S. J., Wei, H., and Chai, H. (2014). "Self-assembled hierarchical graphene/polyaniline hybrid aerogels for electrochemical capacitive energy storage," *Electrochim. Acta* 137, 381-387. DOI: 10.1016/j.electacta.2014.06.017

Zheng, Q., Cai, Z., Ma, Z., and Gong, S. (2015). "Cellulose nanofibril/reduced graphene oxide/carbon nanotube hybrid aerogels for highly flexible and all-solid-state supercapacitors," *ACS Appl Mater & Inter* 7(5), 3263-3271. DOI: 10.1021/am507999s

Zhang, W. J. (2011). "A review of the electrochemical performance of alloy anodes for lithium-ion batteries," *J. Power Sources* 196(1), 13-24. DOI: 10.1016/j.jpowsour.2010.07.020

Zhang, K., Zhang, L. L., Zhao, X. S., and Wu, J. (2010). "Graphene/polyaniline nanofiber composites as supercapacitor electrodes," *Chem. Mater.* 22(4), 1392-1401. DOI: 10.1021/cm902876u

Article submitted: October 21, 2019; Peer review completed: December 8, 2019; Revised version received: January 20, 2020; Accepted: January 21, 2020; Published: January 27, 2020.
DOI: 10.15376/biores.15.1.1828-1843